Atmospheric
Measurement
Techniques
Discussions

AMTD

6, 5297–5344, 2013

Planetary boundary
layer of the urban
area of Rome

E. Pichelli et al.

Title Page

Abstract   Introduction

Conclusions   References

Tables   Figures

◄   ►

◄   ►

Back   Close

Full Screen / Esc

Printer-friendly Version

Interactive Discussion

The role of urban boundary layer investigated by high resolution models and ground based observations in Rome area: a step for understanding parameterizations potentialities

E. Pichelli[1], R. Ferretti[1], M. Cacciani[2], A. M. Siani[2], V. Ciardini[2], and T. Di Iorio[3]

[1]University of L'Aquila/CETEMPS, Department of Physics, L'Aquila, Italy
[2]Sapienza University of Rome, Department of Physics, Rome, Italy
[3]ENEA, UTMEA-TER, Rome, Italy

Correspondence to: E. Pichelli (emanuela.pichelli@aquila.infn.it)

Abstract

The urban forcing on thermo-dynamical conditions can largely influences local evolution of the atmospheric boundary layer. Urban heat storage can produce noteworthy mesoscale perturbations of the lower atmosphere. The new generations of high-resolution numerical weather prediction models (NWP) is nowadays largely applied also to urban areas. It is therefore critical to reproduce correctly the urban forcing which turns in variations of wind, temperature and water vapor content of the planetary boundary layer (PBL). WRF-ARW, a new model generation, has been used to reproduce the circulation in the urban area of Rome. A sensitivity study is performed using different PBL and surface schemes. The significant role of the surface forcing in the PBL evolution has been verified by comparing model results with observations coming from many instruments (LiDAR, SODAR, sonic anemometer and surface stations). The crucial role of a correct urban representation has been demonstrated by testing the impact of different urban canopy models (UCM) on the forecast. Only one of three meteorological events studied will be presented, chosen as statistically relevant for the area of interest. The WRF-ARW model shows a tendency to overestimate vertical transmission of horizontal momentum from upper levels to low atmosphere, that is partially corrected by local PBL scheme coupled with an advanced UCM. Depending on background meteorological scenario, WRF-ARW shows an opposite behavior in correctly representing canopy layer and upper levels when local and non local PBL are compared. Moreover a tendency of the model in largely underestimating vertical motions has been verified.

1 Introduction

Nowadays, numerical weather prediction (NWP) models can work at very high resolutions ($\approx$ km), but there are many sub-grid motions that develop at finer scales and can not be explicitly represented. They have to be included into the models for correctly re-

Planetary boundary layer of the urban area of Rome

E. Pichelli et al.

Title Page

Abstract	Introduction
Conclusions	References
Tables	Figures

|◄ | ►|

◄ | ►

Back | Close

Full Screen / Esc

Printer-friendly Version

Interactive Discussion

producing the atmospheric states. Turbulent mixing is one of the sub-grid phenomena having a large impact on the state of the atmosphere; it occurs within the the first kilometers of atmosphere and it characterizes the planetary boundary layer (PBL), taking charge of the vertical transport of mass, heat and momentum. The relatively high fre-
quency of occurrence of turbulence near the ground differentiates the PBL from the rest of the atmosphere (Stull, 1988). NWP models have to reproduce turbulence at various scales and so they need appropriate representation of PBL. Nowadays, many different PBL schemes are available and they differ by the vertical mixing formulation and the closure order. Some parameterizations have computational advantages (like the ones
based on the so called *local-K* approach), but they can fail in reproducing the mass and momentum transport accomplished by large eddies (Stull, 1993). In order to overcome these deficiencies parameterizations accounting for non local contributions by counter-gradient terms (*nonlocal-K* approach) or more sophisticated representations like higher order closure approaches based on prognostic prediction of turbulent kinetic energy
(TKE) have been developed. Recently, the new generations of high-resolution NWP models have been applied also to urban areas for both weather forecast and research purposes. The urban areas largely influence local evolution of the atmospheric boundary layer as the urbanization represents a significant forcing on thermo-dynamical state. Generally, these areas are covered by dry materials (asphalt or concrete) and are
warmer and drier than adjacent rural areas (Oke, 1982); the efficiency of the urban areas in storing heat can produce remarkable mesoscale perturbations of the lower layers of the atmosphere. Therefore, it is critical to correctly reproduce the urban forcing which turns in variations of wind, temperature and water vapor content of the PBL. Hence, featuring the urban boundary layer adds a further complexity that is usually re-
solved by coupling PBL schemes with urban canopy surface parameterizations inside models. Choosing appropriate physical parameterizations is as important as using accurate initial conditions. In particular the accuracy of the PBL schemes affects forecasts of both local and large scale meteorological phenomena (Hacker and Snyder, 2005). They are as fundamental as cloud and microphysics schemes in forecasting precipi-

tation and in simulating complex structures such as hurricanes (Braun and Tao, 2000; Li and Pu, 2008). The WRF model has many PBL schemes available that have been largely tested for precipitation, but only a few studies investigated the response of different schemes on the prediction of near-surface and PBL properties (Shin and Hong, 2011). In this study two parameterizations of the WRF model, the Yonsei University (YSU, Hong et al., 2006) and Mellor-Yamada-Janjic (MYJ, Mellor and Yamada, 1982), are used to investigate their ability in reproducing meteorological conditions in the urban area of Rome and its surroundings to optimize the model configuration for operational purposes over that area. Previous studies have, moreover, shown the influences of land-surface scheme on the structure of the PBL (Pan and Mahrt, 1987; Stull, 1988). Recently Shin and Hong (2011) concluded that thermodynamical surface variables are more strongly influenced by surface-layer schemes than by PBL ones; based on these considerations also a sensitivity to the surface layer of the two PBLs is investigated to highlight their role in featuring the PBL inside and outside the Rome urban area. As a further step, simulations with different urban canopy models have been performed to investigate their impact on the urban boundary layer representation respect to the standard parameterization of the urban area (bulk approach); Martilli (2002) shows the improvements produced by a non standard urban model on the boundary layer structure, thus assessing the importance of a suitable representation of the urban effects to improve the model forecast. Of course the final choice among urban schemes with different level of sophistication should depend on the purpose of the simulation. Observations of thermo-dynamical PBL parameters from sonic anemometer, LiDAR, SODAR and ground based stations have been used for the comparison here presented. The paper is organized as follows: in Sect. 2 a brief description of instruments and experimental techniques are presented. Meteorological scenario of the case studies is presented in Sect. 3. In Sect. 4 the model configuration and a brief description of parameterizations are illustrated together with the different numerical experiments. Results and conclusive remarks are discussed in Sects. 5 and 6 respectively.

2 Observed data processing

2.1 Sonic anemometry

Sonic anemometry is mainly used in atmospheric turbulence studies. This instrument allows to measure three dimensional wind velocity and sonic temperature. From the latter it is possible to retrieve the virtual air temperature. Sonic anemometer is a totally passive instrument which does not interfere with the fluid motion. The operating principle is that the time lag of the sonic waves propagating in moving air depends on air speed and direction; it measures the "transit time", i.e. the time it takes for ultrasonic signal to travel from one transducer to another. An ultrasonic anemometer (model 81 000 V of the Young Company, USA) was installed in 2007 on the roof of the building of Physics Department within the Campus of Sapienza University of Rome (41.9° N, 12.5° E, 75 m a.s.l.). This place is located in the city center which is a very populated area, strongly influenced by anthropogenic activity (Meloni et al., 2000). The air temperature (Ta) and relative humidity (RH) probes combine thermistors (accuracy: ±0.15 °C; range of measure: −30/50 °C; response time: 20 s) and capacitive hygrometer (accuracy: 3 % in the RH range of 10–100 %). Both meteorological sensors and the sonic anemometer are connected to a data logger. The sampling rate of the anemometer as well as the air temperature and relative humidity is 32 Hz. Horizontal and vertical wind components together with sonic temperature and the RH nand Ta values are sampled every 30 min. Spikes were identified and removed when the readings were above/below ±3.5 std taking into account a temporal window of 100 s. Re-processing software performs a quality control of the data set and provides every 30 min the means of three wind components and their standard deviations, the horizontal mean wind, the mean direction, the mean sonic temperature and its standard deviation. The same for air temperature and relative humidity. In addition some turbulence parameters, such as friction velocity and turbulent heat transfer, are retrieved.

2.2 The LiDAR system

The system has been designed to observe atmospheric aerosol vertical profiles in the boundary layer and the free troposphere. The radiation source is a Q-switched single-stage Nd:YAG laser emitting linearly polarized pulses at 1064 and 532 nm with a repetition rate of 10 Hz. The 532 nm radiation is produced by a 2nd harmonic generator crystal. The backscattered radiation is collected by a 100 mm diameter reflector telescope in a Cassegrain configuration. The laser beam is directed towards the zenith coaxially to the Cassegrain receiver, hence the telescope secondary mirror masks the strong atmospheric echoes from the lower 300 m; in this way, detectors saturation is prevented and the receiver sensitivity and field of view (FOV) is regulated to observe the atmosphere up to the tropopause. Another small-aperture, large-FOV refractor telescope receiver is placed beside the Cassegrain but sufficiently close to the laser beam to observe the strong echo from the lowest atmosphere. The collimated signals are filtered by narrow-band interference filters to reduce the sky light and to allow measurements even in full daylight during the summer. Simultaneous analog detection and single photon counting is performed on the signals received by the larger telescope, while analog detection only is performed on the signal from the smaller receiver. The low range analog signal and the high range analog and photon counting signals are matched in the overlapping altitude ranges to produce a continuous LiDAR signal from about 50 m to the upper troposphere with a vertical resolution of 7.5 m. The acquisition system is programmed to perform an integration of the backscattered signals over 300 laser shots, corresponding to 30 s. This is the highest time resolution achievable from the saved raw data but all the analyses were performed on profiles averaged over 5 min corresponding to 3000 laser shots. The retrieval of the backscatter ratio R, defined as the ratio between the total (aerosol and molecules) backscattered signal, and the portion due to the atmospheric molecules only, is obtained by a standard algorithm. The procedure to estimate the height of the Atmospheric Boundary Layer (PBLH) is based in the computation of three parameters vs. time as follows.

1. Three derived quantities from the profiles of $R(t, z)$, namely TV (time variance), FD (first order derivative in z) and SD (second order derivative in z) are calculated using a 3-point, Lagrangian interpolation along the vertical coordinate. Both FD and SD are smoothed by a running average over 75 m in the vertical (this is the error associated to PBLH. The procedure to achieve the final SD profile requires two smoothing).

2. From the closest-to-the-ground relative maximum in the TV vertical profile a negative maximum in the FD followed by a positive maximum in the SD are searched in a range of 400 m of height. If the search is successful the three heights for TVH, FDH and SDH are saved. If FD and SD maxima are both not found in the previous height interval, the search is moved iteratively to the height interval around the next-in-height TV peak. Hence three altitudes, TVH(t), FDH(t), and SDH(t), are associated to each aerosol profile (i.e. at every time step), and the mixing layer height is calculated as the average between FDH and SDH, that are assumed to represent an estimation of the bottom and top heights of the entrainment zone.

2.3 The SODAR system

The Doppler SODAR is operated in a three-axis monostatic mode with a pulse repetition period of 6 s allowing a maximum probing range of 1000 m. Two antennae are tilted 20° from the vertical, one pointing to north and the other pointing to east, and the third antenna pointing to zenith. The three antennae simultaneously radiate 100 ms long acoustic bursts, respectively centered at 1750, 2000 and 2250 Hz, providing a vertical height resolution of 27 m. A digital signal processor performs the signal analysis in real time. A two-step technique is employed in the determination of radial velocities to minimize the influence of noise on measurements. The vertical wind has a precision of $0.1 \, \text{m s}^{-1}$. More detailed descriptions of the electronics and the Doppler reduction technique are available in literature (Argentini et al., 1992). The vertical profiles of the three components of the wind every 60 s and vertical profiles of the turbulence inten-

sity every 6 s is detected by SODAR. A data processing similar to the one used for the LiDAR is applied to the turbulence intensity profiles to retrieve the height of the mixing layer height.

3 Meteorological description of the event

5 Different meteorological scenarios have been used to investigate the model capability in reproducing local conditions associated with or without large scale signals in the urban area of Rome. The events have been selected also based on the measurements availability as follows: 17–18 January 2008 as *winter case with weak advection and convection*; 6–7 February 2008 as *weak convection case caused by moderate advec-*
10 *tion*; 30 June 2008 as *summer like convection case*.

For readability reasons, only 6–7 February 2008 will be extensively discussed; the two other events are also analyzed, but only remarkable differences/similarities with the one presented will be discussed. To investigate the PBL structure over the urban area of Rome a comparison among the instruments is performed. The following meteoro-
15 logical parameters are used for this analysis: measurements at 25 m of the horizontal wind velocity ($m s^{-1}$) and direction (deg) as well as vertical velocity ($cm s^{-1}$), friction velocity ($m s^{-1}$) by the sonic anemometer and temperature (°C) and relative humidity (%) by combined probes; the PBL height (m) time series retrieved by the LiDAR measurements; the time series of the horizontal and vertical wind profiles measured by the
20 SODAR.

It has to be pointed out that the anemometer is detecting the atmosphere within the canopy layer, whereas SODAR and LiDAR are both scanning the atmosphere above this layer, but within the PBL. Therefore, the anemometer measurements are not directly comparable with the SODAR and LiDAR ones, but coupling the two allows for
25 investigating a large part of the PBL.

The 6–7 February 2008 case is characterized by the transition from a *weak advection* regime to one of *weak convection caused by moderate advection*. Some of the

features of this event are present also in the other cases and they will be briefly pre-
sented later. During 6 February, a low pressure in the south-east of Italy produces
south-eastward weak wind over central Italy, whereas on 7 February the wind speed
increases blowing mainly from east because of an anticyclone rapid incoming from
north-west. This is associated to an outbreak of cold and dry air which triggers weak
but no precipitating convection, destabilizing the lower atmosphere. For this event the
sonic anemometer shows weak wind speed during the first day, except for a maxi-
mum (Fig. 1a) observed at approximately 15:00 UTC; an increase of the wind strength
is observed before midday of the second day, lasting for the whole period. The wind
direction (Fig. 1b) shows a westerly/north-westerly wind during the second part of 6
February, probably produced by the interaction of large scale flow with the on set of the
sea breeze as the timing and the permanence (from 12:00 to 18:00 UTC) of this wind
regime would suggest. Sea breeze interaction with the circulation in the urban area of
Rome is a well established phenomenon even in winter time (Mastrantonio et al., 1994;
Ferretti et al., 2003). During the second day a larger variability is detected; this is asso-
ciated with a north westerly wind, in phase with an updraft registered during 7 February
(Fig. 1c) and an increase of the frictional velocity (Fig. 1d). It has to be pointed out that
anemometer measurements of vertical wind component are affected by large errors;
standard deviation shows values (Fig. 1c, gray bars) comparable with the measure-
ments itself ($\approx 0.5\,\mathrm{cm\,s}^{-1}$). The mean standard deviations taken over the 6–7 February
time series for each anemometer variable are presented on Table 1 and give an idea
of their order of magnitude. Two diurnal updrafts are detected by the anemometer due
to both free and forced convection (Fig. 1c): at approximate 15:00 UTC of 6 February
and at 11:00 UTC of the day after. The first updraft (Fig. 1c, red line at 15:00 UTC of
6 February) is mainly due to buoyancy which is sustained by both thermal contribution
of urban heat island (UHI) and by mechanical contribution as suggested by the friction
velocity increase well in phase with it (Fig. 1d). During the second day larger veloci-
ties are detected for both the horizontal and vertical wind component (Fig. 1a and c,
red line, after 11:00 UTC of 7 February) because of an increase of the instability pro-

Title Page

Abstract | Introduction

Conclusions | References

Tables | Figures

|◄ | ►|

◄ | ►

Back | Close

Full Screen / Esc

Printer-friendly Version

Interactive Discussion

duced by the cold and dry air outbreak; moreover a second updraft is registered after 18:00 UTC of comparable intensity with the diurnal one. This allows for inferring that, during the second day, the horizontal advection is partially inhibiting free convection, but it is contributing to develop local mechanical turbulence.

The PBL height retrieved by LiDAR clearly shows a well developed PBL during the first day (Fig. 2a), supporting the hypothesis of meteorological conditions strongly driven by the local forcing. On the other hand, the large variability and the shallow PBL recorded during the second day (Fig. 2a) confirms a different meteorological regime driven by the large scale circulation.

The updrafts recorded by the anemometer (Fig. 1c) associated to the two PBL height maxima are respectively weaker for the first day and stronger for the second one. This would suggest different energy contributions: during the first day the convective thermal plume develops thanks to the urban heat island and the lack of strong wind also at upper levels (Fig. 3a); during the second day, the wind advection associated to the large scale forcing strongly disable the thermal plume allowing mechanical turning which contributes to the updraft and to the frictional velocity increase. In this case the time series of the horizontal and vertical wind vertical profile detected by SODAR confirm the previous hypothesis. The vertical profile of the horizontal wind speed (Fig. 3a) shows a weak signal during 6 February, between 50 and 300 m of height. After midnight a wind increase is recorded, with a maximum greater than $8\,\mathrm{m\,s^{-1}}$ above 100 m and strong winds reaching $14\,\mathrm{m\,s^{-1}}$ during the second part of 7 February. On the other hand, the vertical wind profile (Fig. 3b) shows positive values for the whole period, except for a downdraft after 12:00 UTC on 6 February.

4 Models configuration

The non-hydrostatic WRF ARW (Advanced Weather Research and Forecasting) model is used for this study; it is a primitive equations model with a terrain following vertical coordinate and multiple nesting capabilities (Skamarock et al., 2008). Four two-way

nested domains are used (Fig. 4) to enhance the resolution over the urban area of Rome and its surroundings. The mother domain is centered at 41.116° N, 11.625° E over the Mediterranean basin and it has a spatial resolution of 21.2 km, three more domain are used with resolution from 7.1 to 0.78 km.

The following model configuration has been used (detailed description of parameterizations and useful references can be found in Skamarock et al. (2008):

- 35 unequally spaced vertical levels, from the surface up to 100 hPa, with a higher resolution in the planetary boundary layer;

- long wave RRTM and short wave Dudhia schemes for radiative transfer processes. Both these parameterizations derive from the MM5 model and are respectively based on Mlawer and Dudhia-Lacis-Hansen schemes;

- Kain–Fritsch cumulus convection parameterization is applied to domains 1 and 2; whereas no cumulus scheme is used for domains 3 and 4;

- Morrison two-moment bulk scheme for microphysics.

Numerical experiments have been performed using different PBL parameterizations and different combinations of PBL schemes with surface models to the aim of both assessing the correct configuration for the urban area of Rome and investigating its local circulation. The following parameterizations are used for boundary layer:

- the Yonsei University (YSU) scheme (Hong et al., 2006); this is the new generation of Medium Range Forecast (MRF, Hong and Pan, 1996) scheme, based on the non local K-theory mixing in the convective PBL (Troen and Mahrt, 1986);

- the Mellor-Yamada-Janjic (MYJ) PBL (Mellor and Yamada, 1982; Janjic, 2002); this is a local 2.5 turbulence closure model, with an upper limit imposed on the length scale that depends on the turbulent kinetic energy (TKE) as well as on the buoyancy and shear of the driving flow.

To account for the surface physics a surface scheme together with a land-surface parameterization is needed. The first computes friction velocities and exchange coefficients that enable the calculation of surface heat and moisture fluxes by the land-surface models. These fluxes provide a lower boundary condition for the vertical transport in the PBL; the land-surface model update the land's state variables. Two different schemes are used for both surface (Skamarock et al., 2008):

– the MM5 surface model based on similarity theory (MO-MM5);

– the Eta surface layer (MOY-MYJ);

and land-surface:

– the MM5 5-layer thermal diffusion scheme (TD-MM5);

– the Noah land surface model (NoahLSM).

To the aim of representing the city scale effects at the mesoscale the NoahLSM is also coupled to a urban canopy model (UCM); a single-layer scheme (UCM1) is coupled with YSU PBL (Kusaka et al., 2001), while a multi-layer model (UCM2) is used with MYJ scheme (Martilli et al., 2002).

In order to highlight the sensitivity of the non-local PBL scheme with respect to the land-surface several simulation using the YSU PBL parameterization are performed: (1) using the TD-MM5 for the land-surface (YSUtd); (2) using Noah land-surface model (YSUNoahNOURB); (3) the same configuration of 2 but adding the urban canopy model (YSUNoahUCM1). The same set of simulations are performed using the local 2.5 turbulence closure MYJ model: (1) the MYJtd using the TD-MM5 for the land-surface; (2) the MYJNoahNOURB using Noah land-surface model; (3) same configuration as 2 but adding urban canopy model (MYJNoahUCM2). In Table 2 a summary of simulations performed with different configurations is shown. Acronyms in the first column will identify each simulation hereafter.

The ECMWF analysis for temperature, wind speed, relative humidity, and geopotential height at 0.25° of resolution are interpolated to the WRF horizontal grid and to

vertical levels to produce the model initial and boundary conditions for all the experiments. All the simulations for the case presented last 48 h starting at 00:00 UTC of 6 February 2008.

5 Simulations results

The model results for 6 February 2008 are compared with the local observations detected in the urban area. The meteorological parameters detected by the sonic anemometer and connected probes are compared with the one produced by WRF extracted at the same level. The PBL height time series retrieved by LIDAR measurements and the time series of the horizontal and vertical wind profiles detected by SODAR are compared with the one produced by WRF at the same location. All the model results are analyzed at the highest resolution (0.78 km). A further comparison with ground meteorological stations in the neighborhood of the urban area is performed.

In this study a different behavior in developing dynamics around the urban area of Rome is found using the two PBL parameterizations for the three events. The MYJ (local) produces shallower PBL than YSU (non local) for moderate advection events in agreement with finding of Shin and Hong (2011). The WRF 2 m temperatures at the highest resolution (not shown) shows that MYJ turns out a warmer and wetter field than YSU outside the urban area, regardless of the season, unless the MM5 5-layer thermal diffusion scheme (TD-MM5) is used. Other studies (Hu et al., 2010) have shown an opposite mean tendency for sites in south-east America for the two parameterizations; this contradiction could be addressed to the particular thermally driven circulation of the urban region nearby the coast in the western Italy discussed in Ferretti et al. (2003), but further experiments should be performed to justify the result. On the other hand an opposite tendency is founds inside the city area mainly during night time in agreement with Hu et al. (2010). Moreover, MYJ shows a horizontal temperature gradient smoother than YSU between the UHI and its surroundings during night time; weakening of the wind intensity is also found in the low Tiber valley. To the aim of investigating

Back | Close

Full Screen / Esc

Printer-friendly Version

Interactive Discussion

the two schemes ability in reproducing the PBL and of better understanding the link between the circulation in the urban area and its surroundings, a detailed comparison between the WRF output and the measurements is presented in the next paragraphs for 6 February 2008.

5.1 6–7 February 2008

5.1.1 Inside the urban area

The comparison between WRF and the anemometer (Figs. 5 and 6 for YSU PBL, Figs. 7 and 8 for MYJ PBL)[1] shows an overall good agreement suggesting a fair model ability in capturing the wind signals, though discrepancies are found. The YSU simulations (Fig. 5) show a poor skill in predicting horizontal wind speeds (Fig. 5a) during the weak advection regime for 6 February, producing an overestimation except for a well reproduced maximum after noon. Even larger errors are found during the wind speed increasing phase for 7 February. The WRF overestimation of horizontal wind can be produced by an excess of forcing of the upper layers dynamic to the urban canopy layer, as the comparison with SODAR vertical profiles would suggest (Figs. 10 and 11). As it will be pointed out later, the YSU wind speed maxima are developed at lower level than the SODAR observed ones, strongly supporting the previous hypothesis. This is also found for the case of 17–18 January 2008, in different meteorological regime. YSU coupled with Noah LSM (Fig. 5a, yellow line) produces the largest errors ($\approx 7.8\,\mathrm{m\,s^{-1}}$) and no improvement is found coupling Noah LSM with urban canopy scheme (YSUNoahUCM1, Fig. 5a, green line). A similar horizontal wind time series and comparable errors respect to observations are found for YSUtd (blue line).

The wind direction (Fig. 5b) is fairly reproduced by all YSU during most part of the simulation, but differences with the anemometer reach $\approx 180°$. During night time (from

---

[1]Anemometer is placed on a roof at 25 m of height; model data are extracted at the same level.

22:00 UTC of 6 February to 06:00 UTC of 7 February), the anemometer measurements (Fig. 5b, red line) show mainly a northwesterly wind, whereas the model produces wind initially coming from north-east (typically associated to night flow of the Tiber valley) and later sharp direction changes (Fig. 5b, blue, yellow and green lines). All YSU simulations, except for the peaks registered after midnight, maintain the flow mainly from north-east, with errors below 90 deg respect to anemometer. Also for the wind direction no relevant differences are found using UCM1 (Fig. 5b, green line).

For what concerns the vertical velocities, the comparison between the YSU simulations and the anemometer (Fig. 5c) shows an overestimation of the mean vertical winds at low levels during most part of the simulation regardless the surface scheme (Fig. 5c, blue, yellow and green lines). The model is able to reproduce changes in the vertical velocity intensities (small during 6 February and large during 7 February), but a time delay of few hours is found in reproducing maxima. The model results are within the measurements error, they vary from few $\mathrm{cm\,s^{-1}}$ up to $0.7\,\mathrm{cm\,s^{-1}}$ respect to the anemometer. A weak sensitivity to surface scheme is found: both YSUtd and YSUNoahNOURB (Fig. 5c, blue and yellow lines) show a fair agreement with measurements during the first day, but partially missing the afternoon updraft. This is probably due to the partial loss of the thermal contribution of the UHI and to an early development of the mechanical one, as the friction velocity would suggest (Fig. 5d). The YSUNoahNOURB (Fig. 5c, yellow line) reduces the variability during 7 February by developing a long lasting updraft from the early morning. The UCM1 activation (Fig. 5c, green line) does not produce remarkable changes.

The comparison between the YSU friction velocity and the anemometer (Fig. 5d) shows a fairly agreement during the first day of weak advection regime, although an anticipation of the 6 February maxima is produced; on the other hand a large overestimation during the second day is found. The frictional velocity overestimation probably helps to balance the excess of horizontal momentum vertical flux from high to low levels by decoupling the canopy layer from above ones. This easily occurs for simulations

Planetary boundary layer of the urban area of Rome

E. Pichelli et al.

Title Page

Abstract | Introduction

Conclusions | References

Tables | Figures

◄ | ►►|

◄ | ►

Back | Close

Full Screen / Esc

Printer-friendly Version

Interactive Discussion

of cases with an intrusion of air mass from higher levels, as SODAR observations show for this event (Fig. 10a).

The comparison between anemometer and WRF temperature and relative humidity (Fig. 6) shows a tendency to underestimate both variables. Poor sensitivity to surface scheme is found for temperature (Fig. 6a); all YSU simulations are in good agreement with the anemometer during the first day but they underestimate the diurnal maximum.

During 7 February, larger differences than the previous day are found and no noteworthy impact is produced by the urban canopy model (Fig. 6b, green line); this is partially expected because non local conditions dominate during the second day. During the night the early development (approximately 2 h) of the minimum, associated to a slower increasing rate of temperature and an earlier decrease of humidity, turns in an underestimation of the second day maximum. Then all simulations anticipate the diurnal maximum and underestimate temperatures with errors ranging between 0 and 4 °C. The relative humidity (Fig. 6b) shows sensitivity to the land surface scheme with underestimations in the maximum larger for Noah LSM than the others (Fig. 6b, yellow and green lines); no improvements are found YSUNoahUCM1 (Fig. 6b, green line). All YSU simulations generally underestimate observed values causing large errors (35–50 %) mainly due to the early outbreak of cold and dry during 7 February.

The comparison between MYJ simulations and the anemometer (Figs. 7–8) show trends similar to YSU ones, but a better agreement with measurements is found for most variables. During 6 February and early 7 February, both MYJtd and MYJNoah-NOURB show a good agreement with the anemometer for the horizontal wind speed (Fig. 7a, orange, black and red lines); in addition, the maximum between 12:00 and 18:00 UTC of 6 February is reproduced on time. On the other hand, an overestimation is found during 7 February also for this scheme, regardless the land-surface scheme used if no urban canopy is activated (Fig. 7a, orange and black lines). It is noteworthy the timing of the moderate regime, whose onset for MYJ is correctly shifted, respect to YSU, from the night time to the early morning of the second day. A maximum error of $6.0\,\mathrm{m\,s^{-1}}$ is found, which is smaller than YSU one. The UCM2 activation (Fig. 7a, pink

line) dramatically reduces the horizontal wind intensities causing an underestimation that partially reduces the error during 7 February, but that turns in a larger discreapncy than MYJNoahNOURB because of the underestimation of wind speed during the weak advection regime.

The MYJ is able to reproduce the wind direction time series fairly well during most part of the simulation (Fig. 7b), but in the early hours of 6 February it misses the sharp changes registered by anemometer as for YSU. During the nighttime, it produces errors similar to YSU with wind coming mainly from east/north-east, whereas the anemometer detected wind from north-west. However, both MYJtd and MYJNoahNOURB show smaller errors than YSU during the last part of the simulation (Fig. 7b, orange and black lines).

A quite good agreement between MYJ and the anemometer vertical wind velocity (Fig. 7c) is found at the beginning of the simulation; this is associated to a better timing than YSU of the 7 February maxima. The local scheme produces larger errors than YSU during last hours of the simulation (≈ 0.6–0.8 cm s^{-1}) because of a time delay in reproducing the nighttime updraft, but an overall better agreement with observations than YSU is found for MYJ. During 6 February an underestimation of the two updrafts developing during the afternoon and night is found for all MYJ simulations (bias ≈ 0.2–0.4 cm s^{-1}). Large sensitivity to the surface schemes is found for MYJ: improvements in reproducing the vertical velocity during the second day is found if the UCM2 is not used (Fig. 7c, orange line for MYJtd and black line for MYJNoahNOURB). The activation of urban canopy model (UCM2, Fig. 7c, pink line) weakens velocities, causing a failure in reproducing the updrafts detected by the anemometer (red line).

The friction velocity for MYJ (Fig. 7d) show trends very similar to YSU ones: a fair agreement is shown during 6 February, beside a time shift in reproducing maxima, whereas an overestimation is found during 7 February. Also in this case poor sensitivity to surface model is found, even if the urban canopy model is used.

The temperature comparison (Fig. 8a) shows that local parameterization (MYJ) also underestimates observations, regardless to the surface scheme but it well reproduces

Title Page

Abstract   Introduction

Conclusions   References

Tables   Figures

◄   ►

◄   ►

Back   Close

Full Screen / Esc

Printer-friendly Version

Interactive Discussion

both cooling and warming rates for both days. Sensitivity to the surface model is found only during the cooling phase on 6 February. If Noah LSM is used (Fig. 8a, black and pink lines) the underestimation increases, mainly if the urban canopy model is activated (Fig. 8a, pink line), thus producing errors larger than YSU ($\approx 0.3\text{–}5\,°\text{C}$). Also for the re-latiqve humidity a better agreement with the anemometer is found for the local scheme than for YSU (Fig. 8b): small errors during both days are found and the maximum is correctly reproduced between 20:00 UTC of 6 February and 06:00 UTC of 7 February. The MYJtd (Fig. 8b, orange line) produces both the smallest underestimation ($\approx 19\%$) during the most part of the simulation and the largest overestimation for the second day minimum ($\approx 18\%$).

The previous analysis allows for inferring a WRF tendency to overestimate horizontal wind component at low levels regardless the PBL parameterization, because of an excess of interaction with the large scale structures. This has been confirmed by the analysis of the two other cases study (not shown) and would suggest an overestimation of vertical transport of horizontal momentum due to an inefficiency in decoupling the canopy layer from the upper ones. In general, coupling the PBL with Noah LSM does not reduce the model error for the wind. A reduction of the wind speed error is found for the local PBL scheme during regimes with upper levels forcing prevailing, if the urban canopy model is used; on the other hand the UCM2 causes a general weakening of vertical winds turning in a large disagreement with measurements. Vice versa, the non local scheme shows poor sensitivity to the urban scheme. Both the parameterizations underestimate temperature during day time at the site height (25 m). The error can be associated to the underestimation of the temperature at lower layers as verified in the comparison with ground based stations shown in next paragraph and in agreement with findings of Hu et al. (2010) for mean diurnal variation of 2 m temperature in south-east American sites. The MYJ temperature shows a larger sensitivity than YSU one to surface and land-surface schemes during the daily cooling phase, also turning in larger errors respect to measurements. On the other hand, the local scheme shows a better ability than YSU in reproducing the evolution of relative humidity in terms of both timing

Title Page

Abstract | Introduction

Conclusions | References

Tables | Figures

◄ | ►◄

◄ | ►

Back | Close

Full Screen / Esc

Printer-friendly Version

Interactive Discussion

and mean values, probably due to a right onset of the large scale signal. The previous results would suggest that the local 2.5 order closure PBL better reproduces the low levels PBL of urban area both for a meteorological scenarios characterized by local circulation and by large scale signal influencing the low levels. In this second case, a multilayer urban canopy scheme allows for reducing the errors for most variables.

To investigate the PBL vertical structure produced by WRF, LiDAR and SODAR measurements are used. LiDAR data provides the PBL height, a key variable inside parameterizations because driving the representation of non local mixing. For this case study PBL height measurements are available by LiDAR and by SODAR for some time interval (Fig. 9, respectively red and black dashed lines). LiDAR measurements (Fig. 9, red line) show a well developed PBL during 6 February reaching a height of 1200 m. During 7 February a lowering of the maximum height is recorded (800 m) associated with a high frequency variability, suggesting a very turbulent state of the atmosphere also during the late afternoon. The large friction velocity values measured by the anemometer support this hypothesis (Fig. 5d, red line).

The PBL height retrieved by SODAR (Fig. 9, black dashed line) is available mostly during night time and early morning; this is usually more accurate than LiDAR one below 500 m (errors never exceeding 75 m); for this event a large agreement between the two instruments is found. The comparison between LiDAR and WRF shows that the model reproduces most likely the PBL growth during the first day, even underestimating and anticipating the maximum regardless the PBL scheme. Besides the time shift, YSUNoahUCM1 (Fig. 9a, green line) produces the largest error for this maximum: a bias of about 500 m respect to observations is found. On the other hand, MYJtd (Fig. 9b, orange line) largely reduce the error to about 90 m. During night time both parameterizations underestimate the height of the PBL and poorly reproduce the signal variability. It is worth to note the ability of both YSU and MYJ to capture the increase of turbulence during early hours of 7 February. The PBL growth during the second day is largely overestimated by both YSU and MYJ. The MYJ (Fig. 9b) anticipates PBL growth on 7 February of approximately six hours; nevertheless it attempts to reproduce the bi-

Planetary boundary layer of the urban area of Rome

E. Pichelli et al.

Title Page

Abstract | Introduction

Conclusions | References

Tables | Figures

◄ | ►►|

◄ | ►

Back | Close

Full Screen / Esc

Printer-friendly Version

Interactive Discussion

Full Screen / Esc

Printer-friendly Version

Interactive Discussion

modal structure recorded by the LiDAR, even producing an overestimation of both the value and the duration of the maxima. It is anyway worth to note that mechanical contributions in MYJ simulations, even overestimated, act to suppress the thermal growth as also found by Martilli (2002) during the day time. On the other hand, the non local parameterizations YSU (Fig. 9a) develops a typical diurnal growth of the PBL producing a large overestimation of the PBL height. During the afternoon (13:00–18:00 UTC) both YSUtd (blue line) and YSUNoahNOURB (yellow line) rapidly decrease the layer height turning in an underestimation of about 300 m of the layer height; in the following hours a new increase of the layer is produced, largely overestimating nighttime height measured by the LiDAR. No improvements are found by using UCM1 (Fig. 9a, green line), except for the correction of the afternoon underestimation to values comparable with the measured ones.

The vertical structure of the PBL is further investigated using horizontal and vertical wind by SODAR (Figs. 10, 11, 12 and 13). On the overall, the comparison between model and observations shows that WRF reproduces fairly well the dynamics occurred during the two days (Figs. 10 and 11). The model overestimates wind intensities and anticipates the wind increase of the second day.

The two PBL produce similar correlations with observed data (0.83 for YSU; 0.84 for MYJ, increasing to 0.85 if UCM2 is used), but some difference is found. The YSU produces the horizontal wind increase a few hours earlier than MYJ (Figs. 10 and 11 respectively) and produces a larger overestimation than MYJ between 06:00 and 12:00 UTC on 7 February. The MYJ better agrees with SODAR data for both the vertical profile variability during the first part of the simulation and for the development of wind speed maxima at higher altitudes than YSU (Fig. 10). This allows for weaker wind below 100 m and for a larger agreement with both SODAR profiles (Fig. 10a) and observations inside the canopy layer (Fig. 7a). Moreover, an upward displacement of maximum is produced by MYJ if UCM2 is activated (Fig. 11d), whereas no remarkable differences are found for YSUNoahUCM1 (Fig. 10d). The further upward displacement induced by UCM2 for MYJ turns in an decrease of the agreement in the first part of the simulation,

but it reduces the bias in the last part. The UCM2 activation correctly reduces the upper levels air intrusion, decreasing the downward transmission of horizontal momentum.

The time series of the vertical profile of the model horizontal wind helps to clarify the hypothesis of a strong link between the canopy layer and the upper levels. This hypoth-
esis was assumed to justify the wind model overestimation respect to the anemometer during second day, except for MYJNoahUCM2 (Figs. 5a and 7a, blue, yellow, green, orange and black lines). This simulation shows as a urban canopy scheme acts to decouple the two layers (Fig. 11d), turning in a reduction of the upper to lower levels forcing and thus producing a better agreement with the anemometer inside the urban
canopy layer during the moderate or strong advection regime (Fig. 7a, pink line).

The vertical wind component by SODAR and WRF are shown in Figs. 12 and 13. To simplify the comparison their color bars are not the same because of the large model underestimation. The SODAR measurements (Fig. 12a) show values ranging between 0 and $80\,\mathrm{cm\,s^{-1}}$; high variability is detected during 6 February: two main updrafts de-
velop between 10:00 and 24:00 UTC, with maxima at 11:00 and 18:00 UTC mostly at upper levels, associated with two weak and short downdrafts after midday.

During 7 February mainly upward motion is detected with two maxima between 01:00 and 05:00 UTC and between 10:00 and 16:00 UTC. The model underestimates vertical motions regardless the PBL parameterization and very low correlation with measure-
ments is found. In addition, WRF shows a long lasting downdraft that is not detected by SODAR during the last part of the simulation. Beside the large underestimation YSU (Fig. 12) better reproduces the observed field than local MYJ (Fig. 13). During 6 February, YSUtd (Fig. 12b) shows a higher variability than MYJtd (Fig. 13b); this last tends to flatten the field during late afternoon suppressing maxima around 18:00 UTC,
as found by the comparison with the anemometer too. On the other hand YSUtd fairly reproduces the signal after 12:00 UTC even if a large bias is found. During 7 Febru-ary, both parameterizations produce large differences with respect to observed data in the last part of the simulation by developing a long lasting downdraft, more intense for MYJ simulations. YSUNoahNOURB (Fig. 12c) weakens winds increasing the er-

Title Page

Abstract | Introduction

Conclusions | References

Tables | Figures

◄ | ►|

◄ | ►

Back | Close

Full Screen / Esc

Printer-friendly Version

Interactive Discussion

ror for updrafts, but partially corrects the field reducing the downdraft; moreover, no significant changes are produced by UCM1 on the YSU simulation (Fig. 12d). The MYJNoahNOURB (Fig. 13c) shows an intensification of the downdrafts with respect to MYJtd, with a consequent increasing of the bias, that is partially recovered by the UCM2 (Fig. 13d). Indeed the MYJNoahUCM2 (Fig. 13d) shows both a shortening of the downdraft in the early afternoon of 6 February and a weakening of the one during 7 February evening.

5.1.2 The suburban area

Twenty ground based stations from SIARL agency[2] are used to investigate the effect of the different PBL on the local and regional circulation. The stations are located in the surroundings of Rome (Fig. 14) and only one of them is inside the urban area (Roma Lanciani). The SIARL stations recorded temperature (T2), relative humidity (RH) at 2 m and horizontal wind speed (WSP) and direction (WDR) at 10 m of height. High correlation values are found between WRF and observations for all meteorological parameters (Table 3), except for wind direction. The YSU shows greater agreement than MYJ for temperature and humidity, with YSUtd reaching the best scores for all variables. The local PBL (MYJ) shows lower correlations than non local one with highest value for TD-MM5 surface (MYJtd). It has to be pointed out, there is only station inside the urban area of Rome, therefore a poor impact is expected for the urban canopy model.

The hourly averaged bias index, calculated as difference between observations and model results, shows a WRF tendency to underestimate observed temperatures (Fig. 15a), except for minima, that are systematically overestimated regardless the PBL scheme and the land-surface model. Bias is similar for the two parameterizations: MYJ produces larger errors than YSU during early 6 February and most part of the second day, whereas it shows better results during nighttime if Noah LSM is used (Fig. 15a, black and pink lines).

---

[2]Servizio Integrato Agrometeorologico della Regione Lazio

The comparison between WRF and observed temperature time series (not shown) at each station shows that WRF systematically anticipates the second day maximum and, consequently, the diurnal cooling phase: this is why a large error is found during that time interval. Errors for relative humidity (Fig. 15b) range between 0 and 30 %: a tendency of the model to underestimate maxima and overestimate minima has been detected; furthermore time series at each station (not shown) highlight a systematic anticipation of the minimum during the second day with larger errors for non local PBL (YSU).

The model shows a general overestimation of the horizontal wind speed (Fig. 15c) increasing after 24 h of simulation, that is during the moderate advection regime. A poor sensitivity to all surface schemes is found for both PBLs. The overestimation for MYJ ($\approx 4\,\mathrm{m\,s^{-1}}$) is smaller than for YSU ($\approx 7\,\mathrm{m\,s^{-1}}$) during the moderate wind phase of 7 February, thus confirming highlights of the comparison with the sonic anemometer (Figs. 5 and 7). A poor influence of urban canopy model activation on suburban area is also found; only small differences (never exceeding $1\,\mathrm{m\,s^{-1}}$) for stations near the urban area (within 15 km, red circle in Fig. 14) are shown respect to simulations without UCM. The bias for wind direction (Fig. 15d) shows that the two PBL parameterizations produce similar errors regardless the surface scheme used. The YSU biases lie within 60° and a small reduction of the error is found if Noah LSM is used. On the other hand the local PBL produces smaller errors (≈ 30 deg) if associated to the thermal diffusion scheme (MYJtd, Fig. 15, orange line).

5.2 Evidences for other cases study

A summary of highlights of the two other cases is presented here. During 17–18 January 2008 weak advection and convection regime occurred. Regardless the PBL parameterization, a model tendency in overestimating weak winds inside the canopy layer if strong wind are produced at upper levels, is confirmed also for this case by the comparison with sonic anemometer. In addition, the vertical profiles time series show that the model develops horizontal wind speed maxima at levels lower than SODAR ones

and it fails in decoupling the low levels from the upper ones. Also in this case the non local scheme (YSU) produces larger errors than MYJ. No remarkable correction is produced for YSU if the urban canopy model is used, whereas a reduction of the horizontal momentum transmission is found for MYJ coupled with UCM2, even turning in an over-

5 all underestimation of wind inside the canopy layer. The temperature and the relative humidity confirms results found for 6–7 February case during the weak wind regime: WRF tends to underestimate the anemometer temperature, showing sensitivity to land-surface scheme in the daily cooling phase, especially if the local PBL (MYJ) is used. Similarly, relative humidity is underestimated by both PBL, but MYJ better reproduces

10 the onset and the duration of the maxima during nighttime. Generally, the comparison between 17–18 January and 6–7 February cases allows for assessing the tendency of the model to produce larger errors, for both thermal and dynamics variables inside the canopy layer, if the circulation is driven by the large scale than by the local one. Finally the comparison with ground based stations in the suburban area confirmed results

15 found for 6–7 February 2008: the model tends to overestimate horizontal wind close to the surface with errors generally larger for YSU than for MYJ. Results for temperature and relative humidity confirms highlights found for 6–7 February 2008 case, except for relative humidity that is generally underestimated. Both PBL show poor sensitivity to UCM models.

20 30 June 2008 is characterized by typical summer condition developing thermal driven convection and sea breeze driven circulation. Results similar to the other cases are found for what concern horizontal wind speed: generally an overestimation is produced for the mean wind. As for the other cases, poor sensitivity is found to UCM1 activation if YSU PBL is used, whereas a weakening of the wind speed is found for

25 MYJNoahUCM2, turning in an underestimation of mean wind observations. The mean vertical velocity are underestimated also at low levels, but it has to be point out that measurements are affected by large uncertainties for this case study. Also in this case, temperature and relative humidity are mostly underestimated with errors respectively larger for MYJ and YSU; on the other hand, MYJ is able to reproduce the high variability

of most variables whereas YSU catches only gross features unless it is coupled with Noah surface. It is worth to note, that this is the only case to show sensitivity to UCM1 if YSU scheme is used: UCM1 reduces the overestimation and delays the maximum of the PBL height as the comparison with LiDAR shows. The comparison with the SODAR

5 shows that in this case the model correctly decouples upper layers from lower ones: the wind maximum is correctly reproduced by the model in terms of both vertical position and wind intensity. Finally, the comparison with surface parameters by ground based stations in the suburban area reveals again the tendency to overestimate horizontal wind velocities. This the only case showing sensitivity to UCM2 for station far from

10 the urban area (outside the 15 km ranged red circle in Fig. 14), but downwind respect to the diurnal sea-breeze. This suggests that the urban canopy model impact also outside the urban area if both low and high levels are dominated by local circulation. On the contrary thermodynamical parameters show poor sensitivity to both land-surface schemes and UCM. Results for temperature confirm a tendency of the model to under-

15 estimate maxima and to overestimate minima, regardless the PBL. On the other hand the comparison for relative humidity confirms a general underestimation of maxima, whereas an opposite tendency between the two PBL in predicting minima is shown: MYJ produce an overestimation, whereas YSU an underestimation.

6 Concluding remarks

20 In this study the WRF model has been used to reproduce the circulation in the urban area of Rome. A inter-comparison of two PBL parameterizations (YSU and MYJ) has been performed to highlight their ability to correctly reproduce the PBL parameters. Moreover, each PBL scheme has been coupled with different combinations of a surface scheme together with a land-surface parameterization to investigate the impact

25 of surface parameters on the PBL evolution. Results from numerical simulation at the highest resolution domain (780 m) have been compared with measurements by a sonic anemometer, a LiDAR and a SODAR. Moreover a comparison of the model with several

rural-based stations has been performed to investigate both the differences between the two PBL and the impact of the urban forcing on the near-surface thermodynamical parameters in suburban areas. Three cases study were selected based on the measurements availability and on their representativeness of typical meteorological

5 scenarios in the Rome area: 17–18 January 2008 is chosen for weak advection and convection conditions; 6–7 February 2008 for the weak convection caused by moderate advection conditions due to the influence of the large scale circulation; finally 30 June 2008 for its typical summer conditions, with local circulation prevailing at both lower and upper levels. Only 6–7 February 2008 has been presented in detail.

10 For what concerns the horizontal wind the comparison with the anemometer revealed a tendency of the model to overestimate its intensity at low levels in both regimes, with larger errors if large scale conditions prevail; the comparison with the SODAR profile pointed out the tendency of the model to develop wind maxima at lower levels than observed, thus suggesting an excess of vertical transport of horizontal momentum

15 from upper to lower levels and an inefficiency in decoupling the canopy layer from the above one. Wind errors respect to observations are greater for YSU than for MYJ both in the weak wind regime and in the moderate one. Poor sensitivity to both surface scheme and urban canopy model is found for YSU, whereas a decoupling of upper and lower layer is shown for MYJ if Noah land surface scheme and multilayer urban canopy

20 model are used. This turns in a good reproduction of the horizontal wind field also in the canopy layer during the moderate wind regime, whereas a slight underestimation is produced during the weak conditions phase.

For what concerns the vertical velocity, WRF agrees with the anemometer within the instrumental error-bars inside the canopy layer, but mean values are overestimated

25 regardless the PBL parameterization. WRF time series are poorly correlated with the anemometer because of time shifting of the maxima; a strong underestimation is found for MYJ if also the urban canopy model is used. Comparison between WRF and the SODAR highlighted large discrepancies for the vertical wind intensities, with error of several $cm\,s^{-1}$ regardless the PBL scheme used; the errors usually increase if Noah

Title Page

Abstract | Introduction

Conclusions | References

Tables | Figures

◄ | ►►

◄ | ►

Back | Close

Full Screen / Esc

Printer-friendly Version

Interactive Discussion

LSM is used. On the other hand using the Noah LSM surface helps to reproduce a more realistic variability of the signals.

A tendency of the model in underestimating temperature and humidity is found if local circulation prevails. MYJ is generally able to correctly reproduce the evolution of diurnal cycle. Time series show a poor sensitivity to different surface schemes, except for MYJ during daily cooling phases, when an increase of the error is found using Noah LSM. Further activation of UCM2 increases the error for temperature minima and humidity maxima in the transition phase between local and large scale circulation.

LiDAR retrieved PBL height shows a layer evolution mainly due to the thermal contribution during weak horizontal advection conditions, whereas also mechanical contributions are found during moderate/strong wind regime due to large scale circulation. The comparison between the model and LiDAR PBL height revealed a model tendency to underestimate the PBL height if YSU is used for thermal prevailing conditions, whereas a good performance of MYJ is found if thermal diffusion surface scheme is used. During the second day, when also a large mechanical contribution occurs, both PBL schemes overestimate the observations, with YSU exceeding the thermal contribution during diurnal hours and MYJ attempting to reproduce the signal variability. A poor sensitivity to surface model is found, confirming a major role played by the mixing algorithms of the PBL parameterizations to the PBL height computation.

The comparison with suburban area stations of two meters temperature and ten meters wind confirmed the model tendency to overestimate wind speed and to produce larger errors if large scale circulation is present at higher levels influencing the lower ones. In this condition, moreover, the YSU errors are larger than MYJ ones. The temperature and humidity are generally underestimated during day time by both parameterizations. On the other hand, during night time YSU underestimates temperature whereas MYJ shows an opposite tendency, because of an underestimation of the cooling rates near the surface. In general a poor sensitivity to the urban canopy model is found for both PBL parameterizations for all parameters recorded by the suburban area stations. This has been found for all cases study, with exceptions for the summer

AMTD

6, 5297–5344, 2013

Planetary boundary
layer of the urban
area of Rome

E. Pichelli et al.

Title Page

Abstract   Introduction

Conclusions   References

Tables   Figures

◄   ►►

◄   ►

Back   Close

Full Screen / Esc

Printer-friendly Version

Interactive Discussion

case. Indeed, when local condition prevail at upper and lower levels, the model is able in decoupling the canopy layer from the upper ones (except for MYJ using Noah LSM). Moreover an impact of UCM2 on the horizontal wind intensity is found for the downwind suburban stations even far from Rome.

References

Argentini, S., Mastrantonio, G., Fiocco, G., and Ocone, R.: Complexity of the wind field as observed by a sodar system and by automatic weather stations on the Nansen Ice Sheet, Antarctica, during summer 1988–89: two case studies, Tellus B, 44, 422–429, 1992. 5303

Braun, S. A. and Tao, W.-K.: Sensitivity of high-resolution simulations of hurricane Bob (1991) to planetary boundary layer parameterizations, Mon. Weather Rev., 128, 3941–3961, 2000. 5300

Ferretti, R., Mastrantonio, G., Argentini, S., Santoleri, L., and Viola, A.: A model-aided investigation of winter thermally driven circulation in the Italian Tyrrhenian coast for a case study, J. Geophys. Res., 108, 4777–4792, 2003. 5305, 5309

Hacker, J. P. and Snyder, C.: Ensemble Kalman filter assimilation of fixed screen-height observations in a parameterized PBL, Mon. Weather Rev., 133, 3260–3275, 2005. 5299

Hong, S.-Y. and Pan, H.-L.: Non local boundary layer vertical diffusion in a medium-range forecast model, Mon. Weather Rev., 124, 2322–2339, 1996. 5307

Hong, S.-Y., Noh, Y., and Dudhia, J.: A new vertical diffusion package with an explicit treatment of entrainment processes, Mon. Weather Rev., 134, 2318–2341, 2006. 5300, 5307

Hu, X.-M., Nielsen-Gammon, J. W., and Zhang, F.: Evaluation of three planetary boundary layer schemes in the WRF model, J. Appl. Meteorol. Clim., 49, 1831–1844, 2010. 5309, 5314

Janjic, Z. I.: Nonsingular implementation of the Mellor-Yamada level 2.5 scheme in the NCEP meso model, NCEP Office Note, 437, 61 pp., 2002. 5307

Kusaka, H., Kondo, H., Kikegawa, Y., and Kimura, F.: A simple single-layer urban canopy model for atmospheric models: comparison with multi-layer and slab models, Bound.-Lay. Meteorol., 101, 329–358, 2001. 5308

Li, X. and Pu, Z.: Sensitivity of numerical simulation of early rapid intensification of hurricane Emily (2005) to cloud microphysical and planetary boundary layer parameterizations, Mon. Weather Rev., 136, 4819–4838, 2008. 5300

Martilli, A.: Numerical study of urban impact on boundary layer structure: sensitivity to wind speed, urban morphology, and rural soil moisture, J. Appl. Meteorol., 41, 1247–1266, 2002. 5300, 5316

Martilli, A., Clappier, A., and Rotach, M. W.: An urban surface exchange parameterisation for mesoscale models, Bound.-Lay. Meteorol., 104, 261–304, 2002. 5308

Mastrantonio, G., Viola, A., Argentini, S., Fiocco, G., Giannini, L., Rossini, L., Abbate, G., Ocone, R., and Casonato, M.: Observations of sea breeze events in Rome and the surrounding area by a network of Doppler sodars, Bound.-Lay. Meteorol., 71, 67–80, 1994. 5305

Meloni, D., Casale, G. R., Siani, A. M., Palmieri, S., and Cappellani, F.: Solar UV dose patterns in Italy, Photochem. Photobiol., 71, 681–690, 2000. 5301

Mellor, G. L. and Yamada, T.: Development of a turbulence closure model for geophysical fluid problems, Rev. Geophys. Space Phys., 20, 851–875, 1982. 5300, 5307

Oke, T. R.: The energetic basis of the urban heat island, Q. J. Roy. Meteorol. Soc., 108, 1–24, 1982. 5299

Pan, H.-L. and Mahrt, L.: Interaction between soil hydrology and boundary-layer development, Bound.-Lay. Meteorol., 38, 185–202, 1987. 5300

Shin, H. H. and Hong, S.-Y.: Intercomparison of Planetary Boundary-Layer Parametrizations in the WRF Model for a Single Day from CASES-99, Bound.-Lay. Meteorol., 139, 261–281, 2011. 5300, 5309

Skamarock, W. C., Klemp, J. B., Dudhia, J., Gill, D. O., Barker, D. M., Duda, M. G., Huang, X. Y., Wang, W., and Powers, J. G.: A Description of the Advanced Research WRF Version 3, NCAR Technical Note, NCAR/TN-475+STR, NCAR, Boulder, CO, USA, 125 pp., 2008. 5306, 5307, 5308

Stull, R. B.: An introduction to boundary layer meteorology, Kluwer Academic Publisher, Dordrecht, the Netherlands, 1988. 5299, 5300

Title Page

Abstract | Introduction

Conclusions | References

Tables | Figures

◀ | ▶|

◀ | ▶

Back | Close

Full Screen / Esc

Printer-friendly Version

Interactive Discussion

Stull, R. B.: Review of non-local mixing in turbulent atmospheres: transilient turbulence theory, Bound.-Lay. Meteorol., 62, 21–96, 1993. 5299

Troen, I. and Mahrt, L.: A simple model of the atmospheric boundary layer: sensitivity to surface evaporation, Bound.-Lay. Meteorol., 37, 129–148, 1986. 5307

Planetary boundary layer of the urban area of Rome

E. Pichelli et al.

Table 1. Anemometer mean standard deviations for 6–7 February 2008; wsp indicates horizontal wind speed, wdr is the horizontal wind direction, w is the vertical wind velocity, u^* is the friction velocity, T is the temperature, RH is the relative humidity.

6–7 Feb 2008	wsp ($m\,s^{-1}$)	wdr (deg)	w ($cm\,s^{-1}$)	u^* ($m\,s^{-1}$)	T (°C)	RH (%)
STD	0.9	29	0.5	0.06	0.2	0.9

Table 2. Outline of performed simulations. On first column the identification acronym of each simulation is shown. On other columns are indicated the parameterizations used (see the text for acronyms).

Simulations	PBL	SURF	LAND-SURF	UCM
YSUtd	YSU	MO-MM5	TD-MM5	Off
YSUNoahNOURB	YSU	MO-MM5	NoahLSM	Off
YSUNoahUCM1	YSU	MO-MM5	NoahLSM	On
MYJtd	MYJ	MOY-MYJ	TD-MM5	Off
MYJNoahNOURB	MYJ	MOY-MYJ	NoahLSM	Off
MYJNoahUCM2	MYJ	MOY-MYJ	NoahLSM	On

Table 3. Correlation values for WRF simulations (rows) respect to SIARL stations for 2 m temperature (T2), relative humidity (RH), horizontal wind speed (WSP), horizontal wind direction (WDR).

| 6–7 Feb 2008	T2	RH	WSP	WDR
YSUtd	0.86	0.77	0.64	0.29
YSUNoahNOURB	0.81	0.73	0.63	0.25
YSUNoahUCM1	0.80	0.73	0.64	0.26
MYJtd	0.75	0.65	0.63	0.34
MYJNoahNOURB	0.71	0.65	0.64	0.30
MYJNoahUCM2	0.72	0.64	0.60	0.32

Full Screen / Esc

Printer-friendly Version

Interactive Discussion
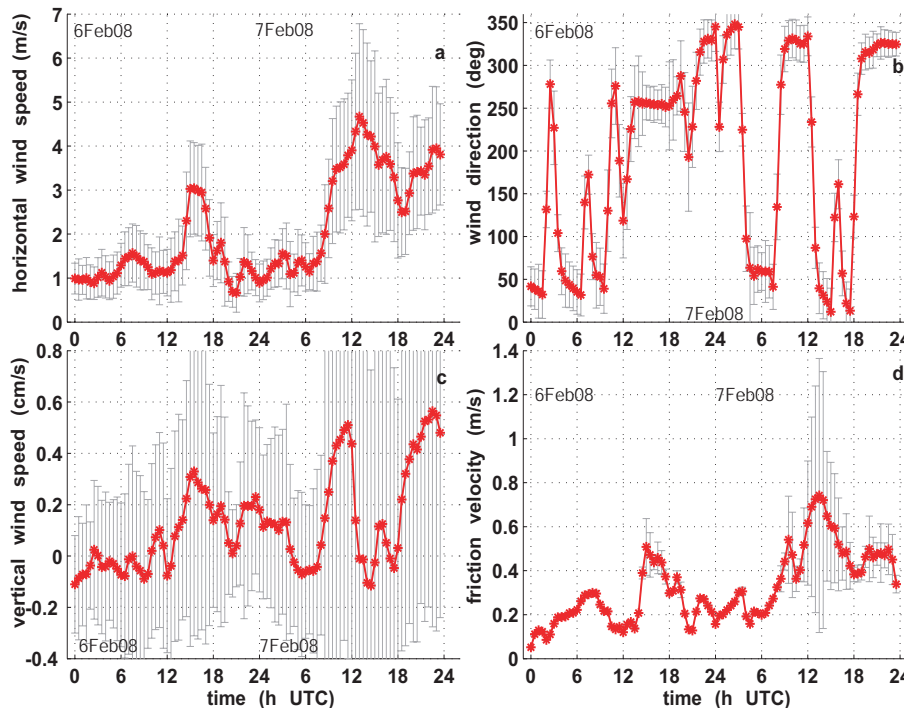
Fig. 1. Time series of horizontal wind speed **(a)**, and direction **(b)**, vertical wind **(c)**, friction velocity **(d)** measured by the sonic anemometer. Standard deviations within the instrumental averaging time are plotted in gray. Observation site is at 41.9° N, 12.5° E; data are measured at 25 m of height.
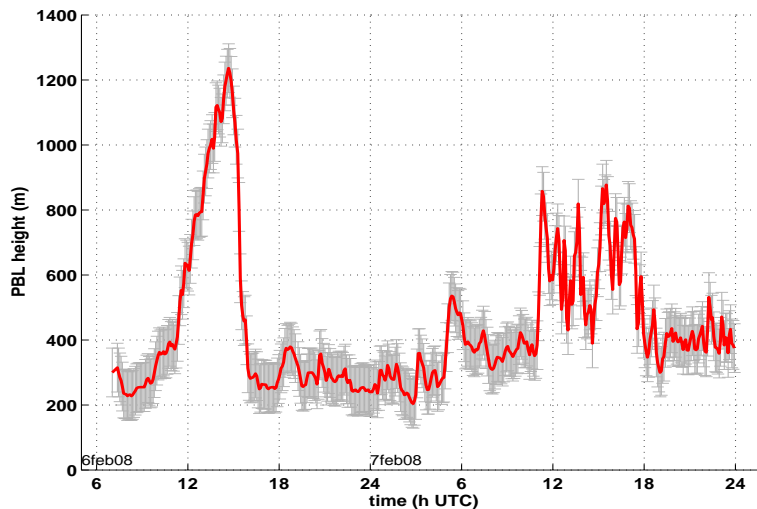
Fig. 2. PBL height time series for 6–7 February 2008 retrieved by the LiDAR (red) and associated errors (grey).
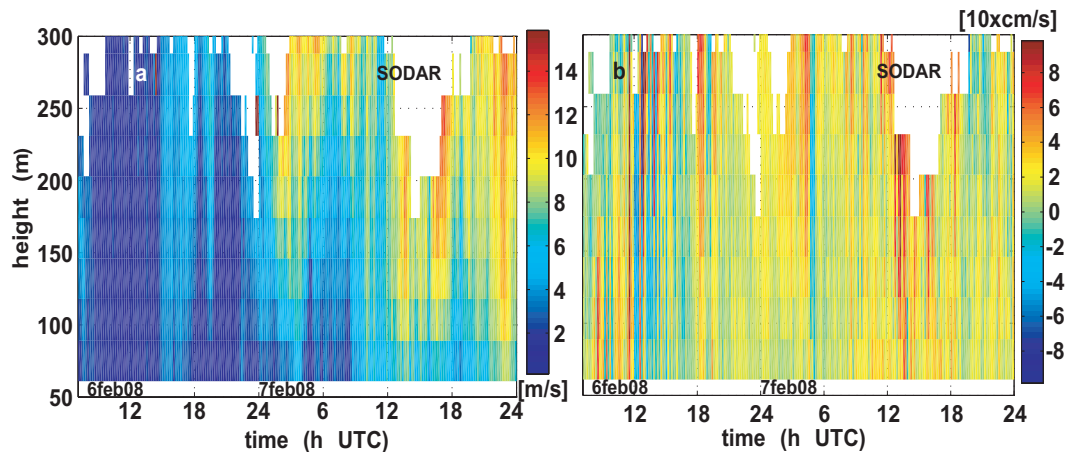
Fig. 3. Time series of the horizontal **(a)** and vertical **(b)** wind speed profile on 6–7 February 2008 measured by the SODAR. Time is on x axis and height on ordinate axis.

AMTD

6, 5297–5344, 2013

Planetary boundary layer of the urban area of Rome

E. Pichelli et al.

Title Page

Abstract   Introduction

Conclusions   References

Tables   Figures

|◄   ►|

◄   ►

Back   Close

Full Screen / Esc

Printer-friendly Version

Interactive Discussion
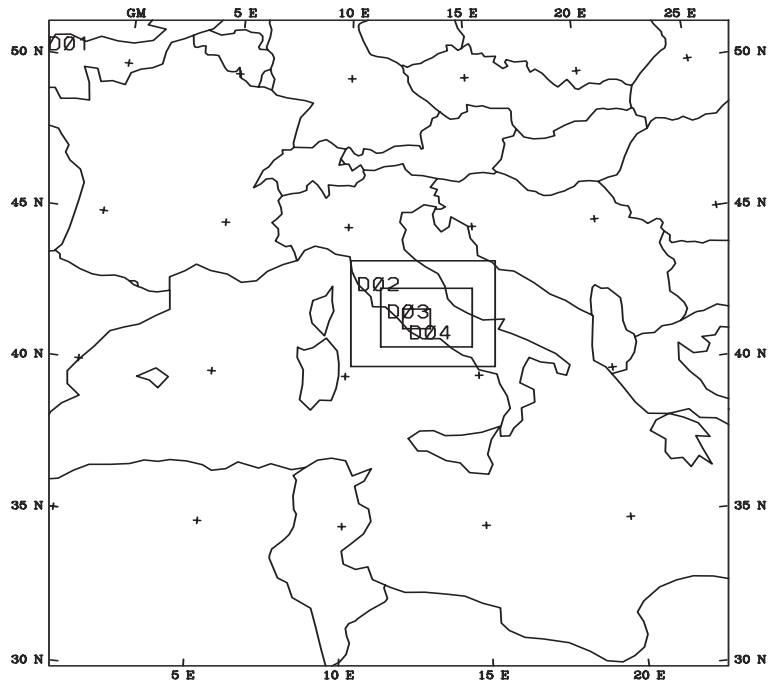
Fig. 4. WRF domains configuration. Domain D1 has resolution of 21.2 km; D2 has resolution of 7.1 km; D3 has resolution of 2.4 km; D4 has resolution of 0.78 km.

Title Page

Abstract | Introduction

Conclusions | References

Tables | Figures

|◄ | ►|

◄ | ►

Back | Close

Full Screen / Esc

Printer-friendly Version

Interactive Discussion
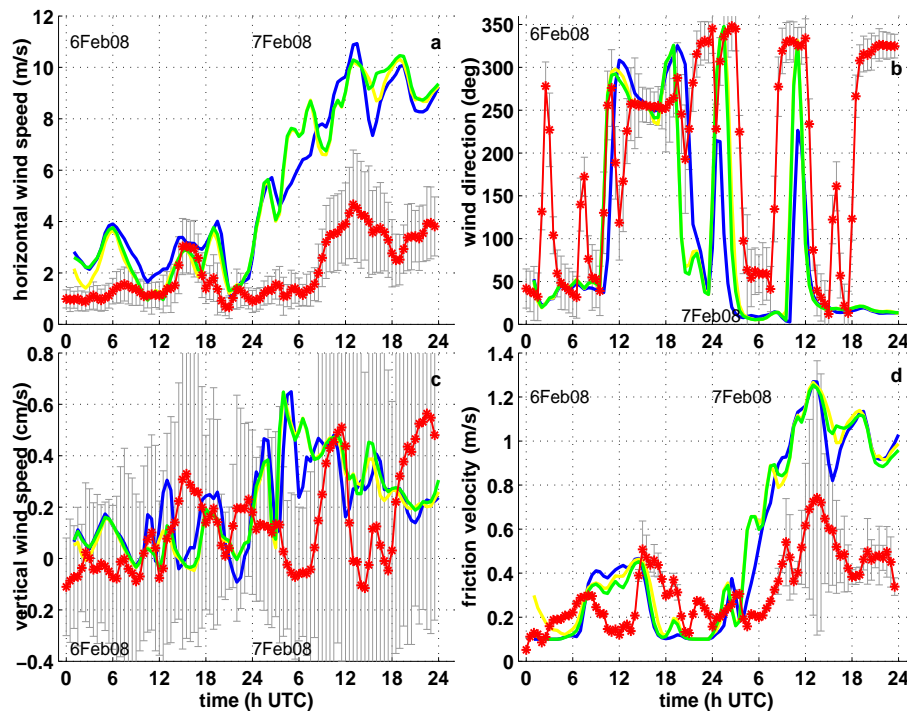
Fig. 5. Time series of horizontal wind speed **(a)**, and direction **(b)**, vertical wind **(c)**, friction velocity **(d)** for 6–7 February 2008. Colours code is: YSUtd (blue); YSUNoahNOURB (yellow); YSUNoahUCM1 (green); anemometer measurements (red) and errors (grey).

AMTD

6, 5297–5344, 2013

Planetary boundary
layer of the urban
area of Rome

E. Pichelli et al.

Title Page

Abstract | Introduction

Conclusions | References

Tables | Figures

|◄ | ►|

◄ | ►

Back | Close

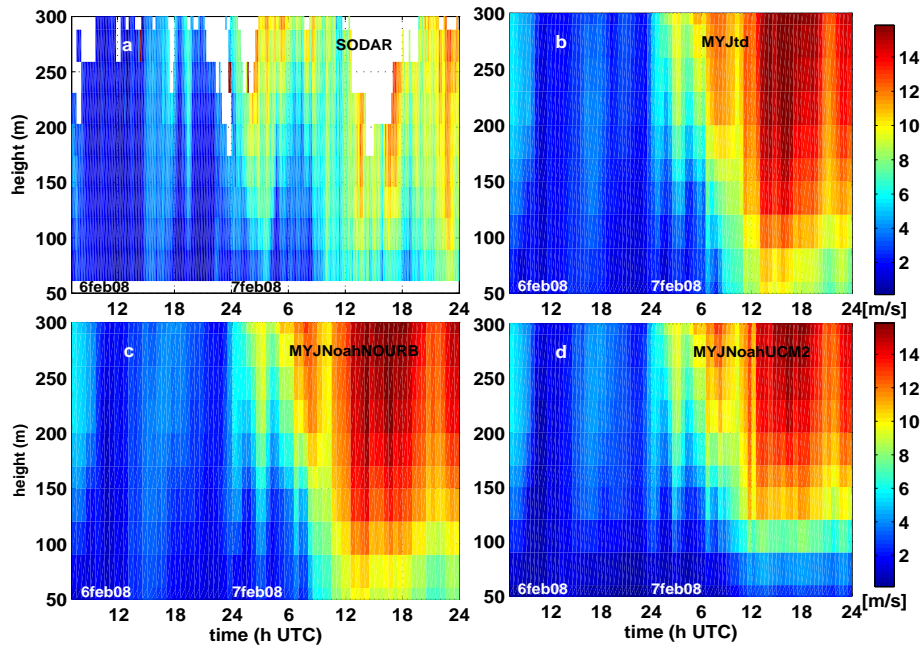Full Screen / Esc

Printer-friendly Version

Interactive Discussion

Fig. 6. Time series for temperature **(a)** and relative humidity **(b)** for 6–7 February 2008. The colour code is: YSUtd (blue); YSUNoahNOURB (yellow); YSUNoahUCM1 (green); measurements by probes combined to the sonic anemometer (red) and errors (grey).

Full Screen / Esc

Fig. 7. Time series of horizontal wind speed **(a)**, and direction **(b)**, vertical wind **(c)**, friction velocity **(d)** for 6–7 February 2008. Colours code is: MYJtd (orange); MYJNoahNOURB (black); MYJNoahUCM2 (pink); anemometer (red).
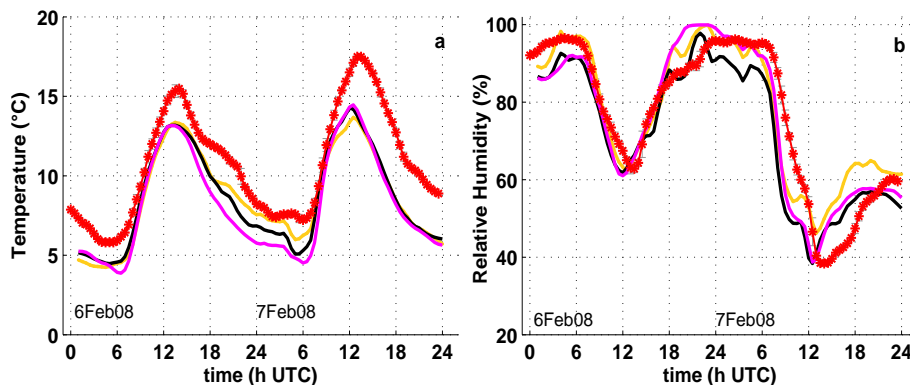
Fig. 8. Time series for temperature **(a)** and relative humidity **(b)** for 6–7 February 2008. The colour code is: MYJtd (orange); MYJNoahNOURB (black); MYJNoahUCM2 (pink); measurements by probes combined to the sonic anemometer (red) and errors (grey).

Title Page

Abstract | Introduction

Conclusions | References

Tables | Figures

|◄ | ►|

◄ | ►

Back | Close

Full Screen / Esc

Printer-friendly Version

Interactive Discussion
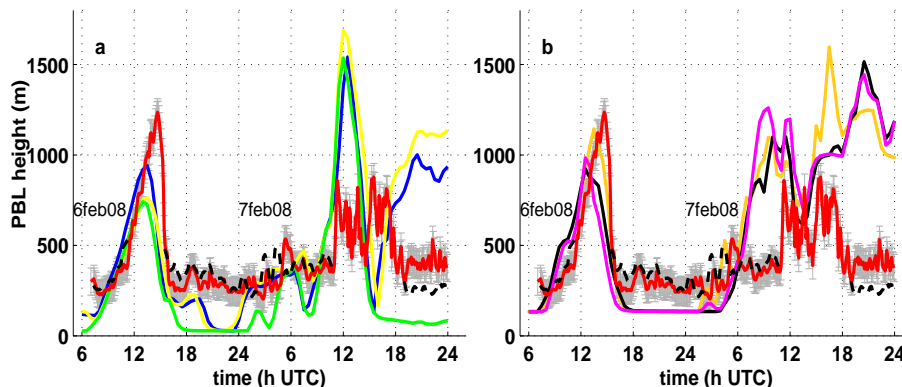
Fig. 9. PBL height time series for 6–7 February 2008 for YSU PBL **(a)** and MYJ PBL **(b)**. The colour code is: YSUtd (blue); YSUNoahNOURB (yellow); YSUNoahUCM1 (green); MYJtd (orange); MYJNoahNOURB (black); MYJNoahUCM2 (pink); LiDAR retrieved PBL height (red) and errors (grey), SODAR retrieved PBL height (black dashed).
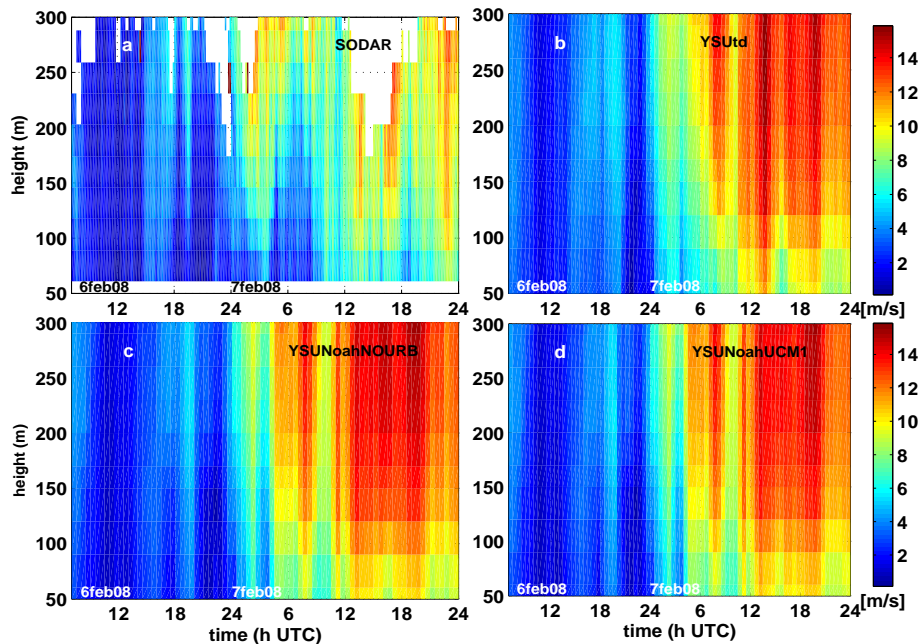
Fig. 10. Time series of the horizontal wind speed vertical profile on 6–7 February 2008 for **(a)** SODAR measurements, **(b)** YSUtd, **(c)** YSUNoahNOURB, **(d)** YSUNoahUCM1. Time is on x axis and height on ordinate axis.

Title Page

Abstract | Introduction

Conclusions | References

Tables | Figures

|◄ | ►|

◄ | ►

Back | Close

Full Screen / Esc
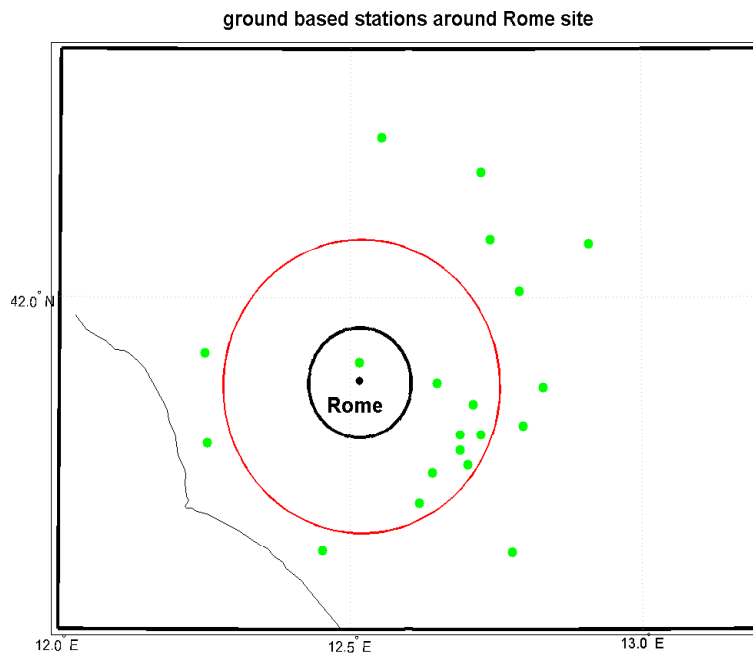
Printer-friendly Version

Interactive Discussion

Fig. 11. Time series of the horizontal wind speed vertical profile on 6–7 February 2008 for **(a)** SODAR measurements, **(b)** MYJtd, **(c)** MYJNoahNOURB, **(d)** MYJNoahUCM2. Time is on x axis and height on ordinate axis.

Fig. 12. Time series of the vertical wind speed vertical profile on 6–7 February 2008 for **(a)** SO-DAR measurements, **(b)** YSUtd, **(c)** YSUNoahNOURB, **(d)** YSUNoahUCM1. Time is on x-axis and height on ordinate axis.
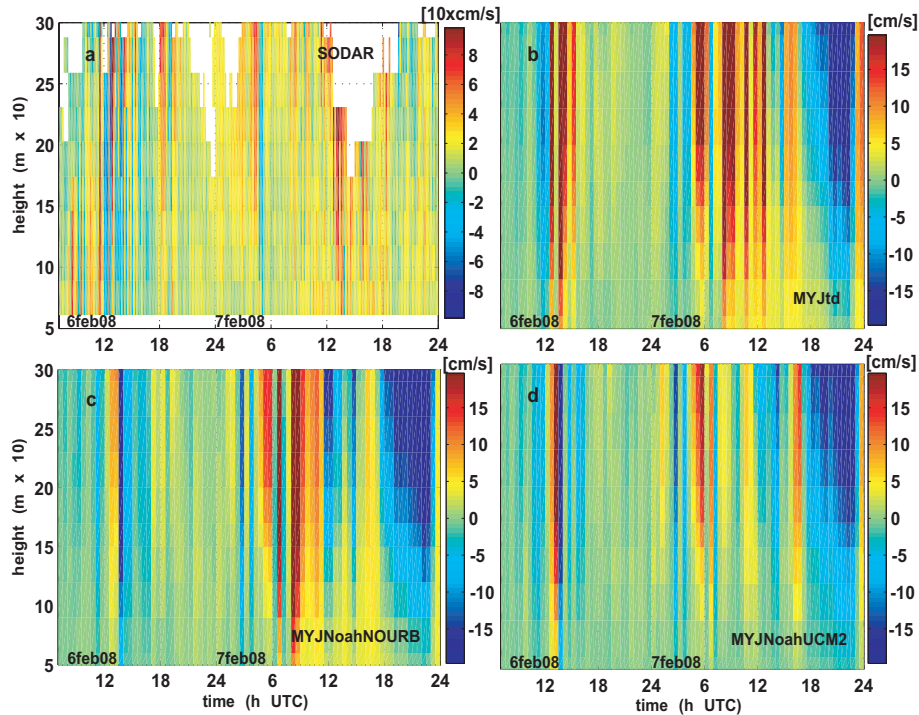
Fig. 13. Time series of the vertical wind speed vertical profile on 6–7 February 2008 for **(a)** SODAR measurements, **(b)** MYJtd, **(c)** MYJNoahNOURB, **(d)** MYJNoahUCM2. Time is on x-axis and height on ordinate axis.
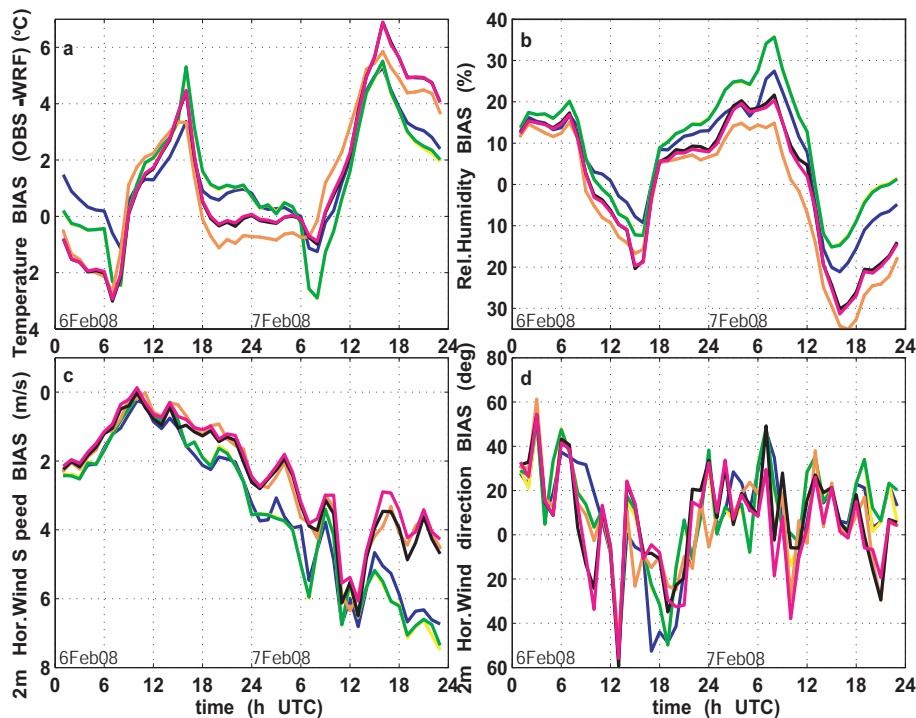
Fig. 14. SIARL stations (green points). The black circled indicates approximately the WRF urban area. The green point inside this area is Roma-Lanciani station. Red circle is the area with stations no more than 15 km far from the city.

Fig. 15. Hourly averaged BIAS between SIARL observations and WRF results for 6–7 February 2008 for **(a)** 2 m temperature (°C), **(b)** 2 m relative humidity (%), **(c)** 2 m horizontal wind speed (m s^{-1}), **(d)** 2 m horizontal wind direction (deg). The color code is: YSUtd (blue); YSUNoahNOURB (yellow); YSUNoahUCM1 (green); MYJtd (orange); MYJNoah-NOURB (black); MYJNoahUCM2 (pink).

Title Page

Abstract | Introduction

Conclusions | References

Tables | Figures

|◄ | ►|

◄ | ►

Back | Close

Full Screen / Esc

Printer-friendly Version

Interactive Discussion